Theory of Periodic Dielectric Waveguides

S. T. PENG, MEMBER, IEEE, THEODOR TAMIR, SENIOR MEMBER, IEEE, AND HENRY L. BERTONI, MEMBER, IEEE

Abstract—**The propagation of electromagnetic waves along open periodic, dielectric waveguides is formulated here as a rigorous and exact boundary-value problem. The characteristic field solutions are shown to be of the surface-wave or leaky-wave type, depending on the ratio of periodicity to wavelength (d/λ). The dispersion curves and the space-harmonic amplitudes of these fields are examined for both TE and TM modes. Specific numerical examples are given for the cases of holographic layers and for rectangularly corrugated gratings; these show the detailed behavior of the principal field components and the dependence of wave-guiding and leakage characteristics on the physical parameters of the periodic configuration.**

I. INTRODUCTION

THIN-FILM structures containing a periodic variation along the film have recently been of considerable interest in integrated optics because of the important role they play in applications such as beam-to-surface-wave couplers, filters, distributed feedback amplifiers and lasers, nonlinear generation of second harmonics, and beam reflection or steering devices of the Bragg type. The periodic variation is usually obtained by means of a dielectric grating, which is superimposed onto the upper surface of a layered configuration. This dielectric grating is in the form of a low-loss layer whose appearance falls into one of two categories: 1) the layer possesses parallel planar boundaries and its periodicity is produced by a longitudinal modulation of its refractive index (e.g., a bleached hologram), or 2) the layer contains a homogeneous medium but its upper boundary has a periodic variation (e.g., a grooved profile obtained by etching). Both types of construction of the dielectric layer are covered by the analysis presented here.

The operation of devices containing a dielectric grating depends on the properties of the electromagnetic fields guided by the structure. These fields appear either as surface waves, which travel parallel to the structure, or as leaky waves, which are guided by the structure but radiate or leak energy continuously into the exterior regions. Both types of waves appear as characteristic (free-resonant) solutions of the boundary-value problem prescribed by the thin-film configurations. Such problems have recently been considered [1]–[14] in the context of several specific structures, but most of the investigations have employed approximations that are too restrictive for many practical cases. The more common approximation has been the assumption that the grating periodicity acts as only a small perturbation in a configuration that, in the absence of the grating, appears as a planar multilayered medium [2], [3], [5], [9], [11], [12]. This approximation yields good results only if the periodic change is sufficiently small, so that its use may produce erroneous results in many practical cases, such as thick corrugated gratings having groove depths comparable to the wavelength [13], [14]. Another approximation has been the use of a Rayleigh assumption which incorrectly neglects the presence of incoming waves in the grating region [2], [4], [8]. It has been shown [10] that this Rayleigh approximation may also result in serious errors if the periodic variation is not sufficiently small. It should also be pointed out that most of the previous studies have developed their analysis in the context of *special* cases, which usually involved not more than three materials or layers; furthermore, some of these studies considered modes having one polarization only (usually the TE type) rather than both TE and TM polarizations.

The aim of this paper is to determine the wave-guiding properties of a very important class of dielectric gratings by utilizing a rigorous approach, which was briefly reported on recently in the specific context of modulated layers [6] and corrugated gratings [13], [14]. This approach does not employ any of the approximations mentioned above and it can be generalized to practically any planar dielectric grating. The generalization is accomplished by first considering both TE and TM modes in a canonic configuration consisting of a periodic layer bounded by two different media; the analysis is thereafter extended to structures with an arbitrary number of layered media, of which the grating configurations examined in the past represent special cases. A similar rigorous analysis has been reported by Neviere *et al.* [10], but their approach requires a numerical integration which may introduce certain inherent disadvantages. Although computer calculations may still be necessary to achieve highly accurate results with the method presented here, their precision can be easily and systematically obtained to any desired order. Furthermore, the solution is already in such a form that it lends itself readily to physical interpretations in terms of the effects due to the individual partial (space-harmonic) fields.

For surface waves and leaky waves supported by dielectric gratings, the two aspects of greatest interest are their dispersion curves and the amplitudes of their space harmonics. The dispersion curves dictate the proper conditions that must be satisfied for effective operation of any optical device employing periodic thin-film waveguides. The space-harmonic amplitudes determine whether the desired interaction is efficient or not. The derivation and calculation of both the dispersion curves and the

Manuscript received April 2, 1974; revised June 17, 1974. This work was supported in part by the U.S. Office of Naval Research, under Contract N00014-67-A-0438-0014, and in part by the U.S. Joint Services Electronics Program, under Contract F44620-69-C-0047.

The authors are with the Department of Electrical Engineering and Electrophysics, Polytechnic Institute of New York, Brooklyn, N.Y. 11201.

space-harmonic amplitudes are therefore presented here in detail, and several numerical examples are given to illustrate their variation with respect to the physical parameters of the periodic configurations. In particular, the role of the grating thickness is discussed and it is shown that the leakage of energy away from the structure is subject to a saturation effect which could not be evaluated by the approximate methods reported in the past.

II. CHARACTERISTIC FIELDS IN THE UNIFORM REGIONS AND THEIR PROPERTIES

The class of periodic thin-film structures considered here is depicted in Fig. 1, which shows structures consisting of one nonuniform (periodic) region and three uniform planar regions. The nonuniform region can be regarded as a planar layer of constant thickness t_g, whose composition varies periodically along x, with period d. The three uniform regions include a thin film of thickness t_f, an upper (air) half space, and a lower (substrate) region. In most practical cases, the substrate thickness is very much larger than the wavelength λ, so that the lower region may also be assumed to be a half space. However, the specific four-regions character of the structures shown in Fig. 1 is chosen here only because of its wide application and the results are generalized later to an arbitrary number of layers. If desired, the finite thickness of the substrate may then also be accounted for.

The fields supported by the structures in Fig. 1 are different in each of the four regions. To find a solution of the electromagnetic problem, it is therefore necessary to consider the type of (characteristic) waves that may appear in every separate region. The solution is then constructed by choosing a suitable combination of these waves so as to satisfy the boundary conditions. We shall therefore discuss here the type of fields that occur in the uniform regions, after which the fields in the periodic (grating) region will be examined in Section III. The boundary conditions and the derivation of the field solution is then given in Section IV, with discussions and numerical examples being presented in subsequent sections.

Because the widths (along y) of all the layers are large with respect to the wavelength λ, the fields are assumed to be invariant with respect to the y coordinate, i.e., $\partial/\partial y = 0$. For simplicity, we also assume that all of the media involved possess the permeability μ_o of air (vacuum) and a time dependence $\exp(-i\omega t)$ is suppressed. If the periodic layer is absent, the field components of characteristic waves in the uniform layers appear in the form

$$F_j(x,z) = F_0^{(j)} \exp\left[i(k_x x + k_z^{(j)} z)\right] \tag{1}$$

where $F_0^{(j)}$ is a constant and

$$k_x^2 + [k_z^{(j)}]^2 = k_j^2 = k_o^2 \epsilon_j. \tag{2}$$

Here $k_o = 2\pi/\lambda$ is the plane-wave propagation factor in air (vacuum) and the index j refers to the jth medium, with $j = a$ (air), f (film), or s (substrate). The quantity ϵ_j is the relative permittivity of the jth medium. In the absence of absorption and scattering losses, uniform layered structures can support surface waves that propagate without attenuation along x and decay away from the

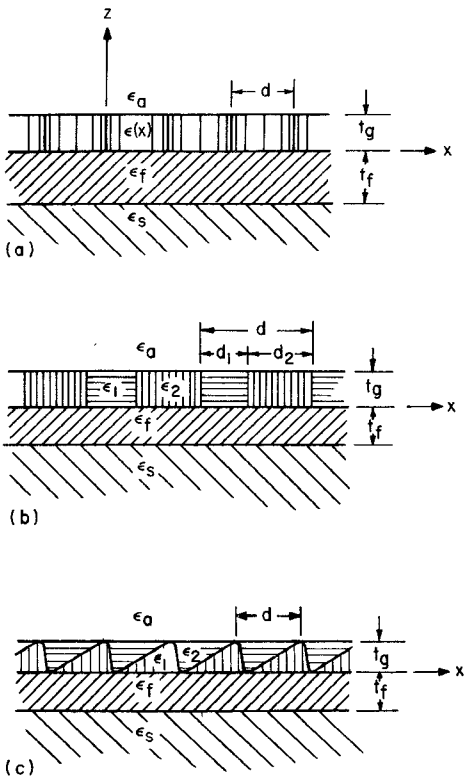

Fig. 1. Varieties of thin-film dielectric gratings. (a) Medium with periodic modulation of its permittivity. (b) Layer with rectangular corrugations. (c) Grating with curved profile.

structure in the air and substrate regions. These waves are therefore characterized by real values of $k_x = \beta_{sw}$ and imaginary values of $k_z^{(j)}$ for $j = a$ and $j = s$.

When a grating is superimposed on the uniform layered structure, the surface-wave field is modified to satisfy the periodic boundary conditions on the grating. Under those conditions, the field in all of the uniform regions (i.e., everywhere except within the grating layer) must appear in the Floquet form

$$F_j(x,z) = \sum_n F_n^{(j)} \exp\left[i(k_{xn} x + k_{zn}^{(j)} z)\right], \qquad (j \neq g) \tag{3}$$

where the amplitudes $F_n^{(j)}$ of each partial field in the above summation can be found by satisfying both the boundary conditions at each interface and the periodic conditions imposed by the grating. The index n under the summation sign is understood to run over all values of $n = 0, \pm 1, \pm 2, \cdots$, this convention being followed throughout this work unless otherwise stated. The quantities k_{xn} are related to the fundamental longitudinal factor k_{x0} by the Floquet condition

$$k_{xn} = k_{x0} + 2n\pi/d, \qquad (n = 0, \pm 1, \pm 2, \cdots). \tag{4}$$

Because $F_j(x,z)$ must satisfy the Helmholtz equation

$$\nabla^2 F_j + k_j^2 F_j = 0 \tag{5}$$

each partial wave now obeys the dispersion relation (2), which yields

$$k_{zn}^{(j)} = \pm (k_j^2 - k_{xn}^2)^{1/2} \tag{6}$$

where the sign in (6) is chosen so that, for real values of k_{x0}, $k_{zn}^{(j)}$ is either positive real or positive imaginary. For complex values of k_{x0}, however, the choice of sign is given by (10), as discussed later.

We observe that each nth partial field in (3) may be regarded as a mode with transverse variation exp $(ik_{xn}x)$ along x, which propagates along z with a propagation factor $k_{zn}^{(j)}$. Hence, within a finite-thickness layer (such as that of thickness t_f in Fig. 1), both signs in (6) must be accounted for because they refer to waves that travel along the $+z$ or the $-z$ directions. In such a case, each nth term in (3) includes two separate components, one each for the $+z$ and $-z$ directions. In the open (air and substrate) regions, on the other hand, it is necessary to retain only that component whose energy flow or decay is away from the structure.

If the grating layer is sufficiently thin, the fundamental propagation factor k_{x0} is very closely given by the propagation factor β_{sw} of the surface wave on the uniform layered structure (with no grating). Also, the fields of the fundamental $(n = 0)$ partial wave are evanescent with respect to z in the air and substrate regions. However, even a very thin grating requires the presence of all k_{xn} to satisfy the appropriate boundary conditions; for such a thin grating, all higher $(n \neq 0)$ coefficients $F_n^{(j)}$ generally possess very small magnitudes. Nevertheless, some of these higher order partial waves may modify the nature of the guided waves. This is seen from (6) where, if we assume that $k_{x0} = \beta_{sw}$, we find that $k_{zn}^{(j)}$ may be real for $j = a,s$ if n is negative and the periodicity length d is sufficiently small. In the air and substrate regions, a real value for $k_{zn}^{(j)}$ implies that the nth field component propagates along z, in contrast to the fundamental ("surface-wave") component $n = 0$ which is evanescent along z. The propagating nth component accounts for energy that flows away from the structure, so that the complete field given by (3) is then no longer a true surface wave because now not all of the energy flows parallel to the x direction.

The foregoing features may be clarified by considering a surface wave incident from the left on a uniform structure, as shown in Fig. 2. For $x > 0$, a grating is superposed on the structure but we may first assume that this grating

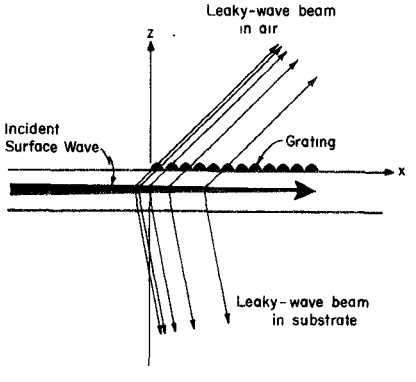

Fig. 2. Surface wave incident from a uniform region $(x < 0)$ onto a region containing a periodic perturbation $(x > 0)$. The periodicity modifies the surface-wave field by leaking beams at angles $\theta_n^{(j)}$ in the air and substrate regions $(j = a, s)$. For clarity, only one such beam is shown in each region. The arrows suggest energy flux.

consists of very small periodic perturbations of the layer that supports the surface wave. Hence, as the surface wave enters into and progresses along the grating portion, a very small amount of field scattering occurs at every perturbation. Because this scattering is very weak, the surface-wave field in the grating region is, on a local scale, essentially quite similar to that in the nonperiodic $(x < 0)$ portion. However, if the grating region is long, the energy leaked by scattering adds up to a large portion of the energy brought into the grating region by the incident surface wave. Because of the regular placement of the scatterers, the individually scattered fields interfere constructively only along certain preferred directions and the leaked energy appears in the form of beams that radiate at angles $\theta_n^{(j)}$, which are given by

$$\tan \theta_n^{(j)} = k_{xn}/k_{zn}^{(j)}. \tag{7}$$

Here $\theta_n^{(j)}$ is a real angle only for real values of $k_{zn}^{(j)}$. Along these real angles $\theta_n^{(j)}$, an energy flux appears in the form of radiation in the air $(j = a)$ or in the substrate $(j = s)$ regions.

The foregoing argument implies that, because energy loss occurs due to radiation, the complete guided field must decay with x as it progresses along the grating region. Hence, the propagation factor k_{x0} along the grating region cannot remain purely real but, instead, k_{x0} is changed from the value β_{sw} of the surface wave to a complex value. We therefore obtain

$$k_{xn} = \beta_n + i\alpha = (\beta_0 + 2n\pi/d) + i\alpha \tag{8}$$

where the imaginary term $\alpha > 0$ is responsible for the decay due to radiation leakage. We note that (8) indicates that the longitudinal decay factor α is the same for all of the partial field components in (3), as required by the Floquet condition (4). Evidently, (6) implies that $k_{zn}^{(j)}$ is then also complex, so that

$$k_{zn}^{(j)} = \xi_n^{(j)} + i\eta_n^{(j)}. \tag{9}$$

We now note that, unlike α, the transverse decay factor $\xi_n^{(j)}$ is generally different for every n. It is also important to recognize that α is small in the case of thin gratings (i.e., small periodic scatterers), but η_n may be large or small depending on n. Because $k_{zn}^{(j)}$ is complex, the square-root sign in (6) must be selected to satisfy[1]

$$\eta_n \gtrless 0 \quad \text{as} \quad \beta_n \gtrless 0. \tag{10}$$

Because waves guided by periodic structures generally contain radiating field components, these waves are no longer true surface waves (with k_{x0} = real). Instead, they are referred to as leaky waves (with k_{x0} complex). Although these leaky waves were described above in terms of small periodic perturbations, it should be evident that the foregoing argument also holds for large periodic scatterers because the size of the perturbations affects the leaky waves only quantitatively. Thus the leakage parameter α and the higher order $(n \neq 0)$ amplitudes $F_n^{(j)}$ are small only in the case of small perturbations; as the size

[1] This choice requires an analytical continuation argument for k_{xn}, as discussed in [25].

of the scatterers increases, α and $F_n^{(j)}$ generally also increase and the overall leakage effect becomes more pronounced.

III. CHARACTERISTIC FIELDS IN THE GRATING REGION

To find the fields supported by the entire thin-film structure, it is necessary to examine the characteristic waves in the periodic layer, which will be henceforth referred to as the grating region. As two-dimensional (y-invariant) fields can be decomposed into TE and TM modes, the Maxwell equations for the field vectors can be reduced to the scalar equation

$$\nabla^2 F_g + k^2(x) F_g = 0 \tag{11}$$

where now $k^2(x)$ is no longer a constant as in (5). We shall restrict the present discussion to gratings of the type shown in Fig. 1(a) and (b), for which $k^2(x)$ is a function of x only. The procedure for extending our results to the more general case having also a z dependence, as is the case in Fig. 1(c), is discussed later in Section IIIC. The electric and magnetic fields $\boldsymbol{E}$ and $\boldsymbol{H}$, and the parameter $k(x)$ are then specified as follows.

TE modes:

$$\boldsymbol{E} = \boldsymbol{y}_o F \quad \text{and} \quad \boldsymbol{H} = -\frac{i}{\omega\mu_o} \nabla \times \boldsymbol{E} \tag{12}$$

$$k^2(x) = k_o^2 \epsilon(x). \tag{13}$$

TM modes:

$$\boldsymbol{H} = \boldsymbol{y}_o \epsilon^{1/2}(x) F \quad \text{and} \quad \boldsymbol{E} = \frac{i}{\omega\epsilon(x)} \nabla \times \boldsymbol{H} \tag{14}$$

$$k^2(x) = k_o^2 \epsilon(x) - \frac{3}{4}\left[\frac{\epsilon'(x)}{\epsilon(x)}\right]^2 + \frac{\epsilon''(x)}{2\epsilon(x)}. \tag{15}$$

Here $\boldsymbol{y}_o$ is a unit vector along y and $\epsilon(x)$ denotes the relative permittivity in the grating region, whose x-dependent behavior is discussed further below in the context of specific examples.

As indicated by (11)–(15), a key step in finding the characteristic solution $F_g = F_g(x,z)$ in the grating region requires the specification of $k(x)$ via $\epsilon(x)$. Because $\epsilon(x)$ is periodic, $k(x)$ can be generally represented by a Fourier series such that

$$k^2(x) = k_o^2 \sum_n p_n \exp(i2n\pi x/d) \tag{16}$$

where the coefficients p_n are known for a given grating. We may then take

$$F_g = \sum_n q_n(z) \exp(ik_{xn}x) \tag{17}$$

where k_{xn} was defined in (4). Inserting this representation into (11), we obtain the system of differential equations

$$\frac{d^2}{dz^2}\boldsymbol{q} = -\boldsymbol{P}\boldsymbol{q} \tag{18}$$

where $\boldsymbol{q} = \boldsymbol{q}(z)$ is a column vector with elements $q_n(z)$ and $\boldsymbol{P} = (P_{nl})$ is a constant matrix (independent of z) whose elements are defined by

$$P_{nl} = k_o^2 p_{n-l} - k_{xn}^2 \delta_{nl}. \tag{19}$$

The system of differential equations (18) characterizes the couplings between all of the space harmonics in the grating region. As a result of this coupling, the variation with respect to z of the waves is considerably more complicated in the grating region than in any of the uniform layers. To solve the coupled system of differential equations with constant coefficients, we may assume a solution of the form

$$\boldsymbol{q} = \boldsymbol{c} \exp(i\kappa z) \tag{20}$$

where κ is a propagation constant along z in the grating region, and $\boldsymbol{c}$ is a constant vector (independent of z). Substituting (20) into (18), we obtain system of linear homogeneous equations

$$\boldsymbol{P}\boldsymbol{c} = \kappa^2 \boldsymbol{c} \tag{21}$$

which states that κ^2 is an eigenvalue of the matrix $\boldsymbol{P}$. We therefore obtain the characteristic equation

$$\det[\boldsymbol{P} - \kappa^2 \mathbf{1}] = 0 \tag{22}$$

where 1 is a unit matrix of infinite order. Let κ_m^2 be an eigenvalue determined from (22); the corresponding eigenvector $\boldsymbol{c}_m$ (with elements c_{mn}) can then be obtained by solving the system of linear homogeneous equations (21). From (20), we thus have a pair of eigensolutions

$$\boldsymbol{q}_m^{(+)}(z) = \boldsymbol{c}_m \exp(i\kappa_m z) \tag{23a}$$

$$\boldsymbol{q}_m^{(-)}(z) = \boldsymbol{c}_m \exp(-i\kappa_m z). \tag{23b}$$

The sign of κ_n is chosen according to (9) and (10). Thus the + and − signs in $q_m^{(\pm)}(z)$ represent waves that travel along the positive and negative directions of the z axis, respectively.

An inspection of the matrix $\boldsymbol{P}$ reveals that the determinant in (22) is of the Hill type, so that the eigenvalues κ_m^2 may be evaluated by a judicious truncation of the determinant. By extending to the present case a theorem on infinite determinants [15], we find that such a truncation is valid provided

$$(1/k_o^2)\,|\,k_o^2 p_o - k_{xn}^2 - \kappa^2\,| > \sum_i{}' |\,p_i\,| \tag{24}$$

which must hold for $|\,n\,| > N$, where N is a finite positive integer and the prime in the summation indicates that the term $i = n$ is excluded. Because the left-hand side in (24) is proportional to n^2 for large $|\,n\,|$ and the right-hand side is independent of n, the above sufficient condition is satisfied if the Fourier series in (16) converges absolutely. If this condition is not satisfied, other mathematical techniques for determining the characteristic solutions in the grating region have to be employed. For example, for gratings of the types shown in Fig. 1(b) and (c), we may resort to the solution of a boundary-value problem for an individual cell of length d, as referred to in Section IIIB.

We recall that the vector $\boldsymbol{c}_m$ contains elements c_{mn}, so that every complete (modal) mth solution F_g in the grating region contains an infinite set of space harmonics, each of which has an amplitude c_{mn}. This is in contrast to

the fields F_j in the other (uniform) regions ($j \neq g$) wherein every nth mode contains a single space harmonic, which forms by itself an independent solution of the pertinent wave equation. After determining the values of κ_m from (22), all of the coefficients c_{mm} can also be found by using (21) which specifies these coefficients as ratios with respect to one of them, say c_{mn}. The value of c_{mm} can itself be prescribed by a normalization condition, which may be chosen to be $c_{mm} = 1$ for the present class of problems. However, it is important to recognize that all κ_m and c_{mn} can be found and may be assumed known if $\epsilon(x)$ is specified in (11)–(15).

To illustrate the foregoing concepts, we shall consider the specific grating structures shown in Fig. 1, which are of current practical interest.

A. Sinusoidally Modulated Medium

For the periodic layer of holographic type, which appears in the structure of Fig. 1(a), a canonic description of its medium is given by

$$\epsilon(x) = \epsilon_g \left(1 + M \cos \frac{2\pi}{d} x\right) \tag{25}$$

where ϵ_g is the average relative permittivity and M is the modulation index.

The propagation of TE waves in such a medium has been extensively investigated by Tamir *et al.* [16]; in this case, the Hill's determinant yielding κ_m and the Fourier coefficients c_{mn} can be conveniently analyzed in terms of rapidly convergent continued fractions. The results have then been applied by Wang [17] to the solutions of TE waves guided by a slab of the modulated medium in a uniform and symmetric environment.

For TM waves, on the other hand, the Hill's determinant has been analyzed by Yeh *et al.* [18], but the harmonic amplitudes c_{mn} have not been studied. Recently, a new formulation for this TM-wave problem has been presented by Peng and Hessel [19]. This new method of analysis is particularly useful for analytically determining the space-harmonic amplitudes c_{mn} of the electromagnetic fields. Thus the boundary value problem for this class of dielectric waveguides can now be rigorously treated for TM waves, in a manner analogous to that of TE waves.

B. Rectangularly Modulated Medium

The variation of the medium that forms the grating in Fig. 1(b) can be described by a rectangular modulation, which is given by

$$\epsilon(x) = \epsilon_1 + (\epsilon_2 - \epsilon_1) \sum_l [U(x - ld) - U(x - ld - d_1)] \tag{26}$$

where $U(x)$ is the unit step function of argument x. In current practice, $\epsilon_1 = \epsilon_a$ and $\epsilon_2 = \epsilon_f$, but we shall here let both ϵ_1 and ϵ_2 be arbitrary so as to cover a larger class of applications.

If the thickness t_g of the grating region is made infinitely large, we obtain a periodic array of dielectric slabs, whose characteristic waves have been examined by Lewis and Hessel for TM modes [20]. In this case, both the dispersion relation for obtaining κ_m and the harmonic amplitudes c_{mn} can be found in terms of closed-form solutions. Hence the solution of the set of equations (21) and their associated Hill's determinant (22) can be dispensed with and the closed forms derived by Lewis and Hessel may be used instead.

Although TE modes have not been explicitly examined by Lewis and Hessel, their analysis is analogous to that of TM modes. Thus, for structures with rectangular corrugations of the type shown in Fig. 1(b), the characteristic waves that appear in the grating region are known, as was also the case for structures with a sinusoidally modulated layer.

C. Curved-Profile Gratings

Because the foregoing two grating profiles possess functions $\epsilon(x)$ that are invariant with z, they lend themselves directly to a rigorous solution of the boundary-value problem. In contrast, the curved profile of Fig. 1(c) is generally not separable with respect to the x and z coordinates and has been solved, so far, only by employing numerical integrations [10]. Nevertheless, the approach described here can be generalized to also solve curved profiles by using judicious approximations of these profiles.

To illustrate this generalization, consider the grating with slanted boundaries in Fig. 3(a). By partitioning the grating into fine layers and approximating each of these by rectangular profiles, we obtain a configuration as indicated in Fig. 3(b). Although now we have more than a single periodic layer, each one of them has a rectangular shape like that in Fig. 1(b) and, furthermore, all of the layers have the same periodicity d. The analysis of the multiply layered grating then follows as a straightforward extension of that for the single grating, as discussed in Section VB. Although this extension is only an approximation for the original slanted grating, this approximation can be made as accurate as desired by subdividing the grating into sufficiently many fine layers.

A much simpler, but probably less accurate, procedure for treating a curved-profile grating is to average (for

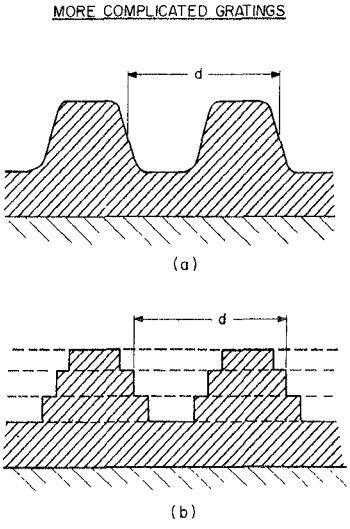

Fig. 3. Approximation of a curved profile by periodic layers with rectangular shapes. (a) Actual profile. (b) Approximated profile.

every x) the permittivity over z inside the grating layer. Thus, if the profile of the periodic boundary that separates the two media with permittivities ϵ_1 and ϵ_2 in Figs. 1(c) or 3(a) is described by the function

$$z = h(x) = h(x + d), \qquad \text{for } 0 \leq z \leq t_g \tag{27}$$

the averaged permittivity becomes

$$\epsilon(x) = \epsilon_2 + (\epsilon_2 - \epsilon_1)\frac{h(x)}{t_g}. \tag{28}$$

The problem is then reduced to that of a layer with uniform thickness but with varying $\epsilon(x)$, as was the case of the modulated medium in Section IIIC above, except that $\epsilon(x)$ in (28) may contain many sinusoidal terms. Nevertheless, this problem lends itself to the same treatment involving Hill's functions as the TM modes discussed by Yeh *et al.* [18] and Peng *et al.* [19].

IV. FIELD SOLUTION FOR PERIODIC LAYERS

After specifying the fields within the separate layers of a dielectric grating structure, we may now consider the boundary-value problem. For this purpose, we simplify the problem by considering first a single periodic layer adjacent to two half spaces, as shown in Fig. 4. In this case, a single periodic layer of thickness t_g is left. The presence of one (or more) uniform layers is then accounted for in Section V by straightforward modifications of the formal rigorous solution of the electromagnetic problem posed by Fig. 4.

Within the periodic (grating) layer, (17) and (23) imply that the electric and magnetic field components transverse to z are, respectively, given by

$$E_g = \sum_m [g_m^{(+)} \exp(i\kappa_m z) + g_m^{(-)} \exp(-i\kappa_m z)] \sum_n V_{mn} \exp(ik_{xn}x) \tag{29}$$

$$H_g = \sum_m [g_m^{(+)} \exp(i\kappa_m z) - g_m^{(-)} \exp(-i\kappa_m z)] \sum_n I_{mn} \exp(ik_{xn}x). \tag{30}$$

The above is a modal representation that regards the fields in terms of modes that propagate in the z direction, each mth term in the first summation being an independent mode with amplitudes $g_m^{(\pm)}$ that are to be determined. Because E_g and H_g are normal to the propagation (z) direction, they correspond to either F_g, discussed in Section III, or to its partial z derivative, depending on which of the specific TE or TM modes are considered.

For any given $\epsilon(x)$ and for an assumed value of k_{x0}, all of the quantities κ_m are known in accordance with the discussion in Section III. Here V_{mn} and I_{mn} refer to voltage and current amplitudes of space harmonics, respectively, one set of which is identical to the set of coefficients c_{mn} forming the vector c_m discussed in Section III; thus, for TE modes we have $c_{mn} = V_{mn}$, whereas for TM modes $c_{mn} = I_{mn}$. The other set is related to the first set via Maxwell's equations, which yield

$$V_{mn} = \sum_r Z_{m,n-r}^{(g)} I_{mr} \tag{31}$$

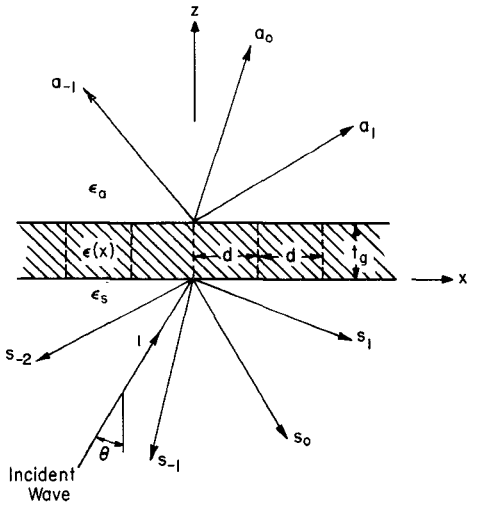

Fig. 4. Canonic configuration containing a single periodic layer of thickness t_g.

where $Z_{m,n-r}^{(g)}$ is an impedance that represents the coupling of the rth harmonic of the magnetic field to the nth harmonic of the electric field. The value of $Z_{m,n-r}^{(g)}$ is determined by the specific relationship that relates E_g and H_g for each mode via Maxwell's equations (12) and (14). For example, in the case of a sinusoidally modulated layer of the type discussed in Section IIIA, we get

$$Z_{m,n-r}^{(g)} = \begin{cases} [\omega\mu_o/k_{zm}^{(g)}]\delta_{nr}, & \text{for TE modes} \\ [k_{zm}^{(g)}/\omega\epsilon_o\epsilon_g][\delta_{nr} + M(\delta_{n-1,r} + \delta_{n+1,r})], & \text{for TM modes} \end{cases} \tag{32}$$

where δ_{nr} is Kronnecker's delta function. For convenience, we assume now that we wish to solve the fields due to a plane wave incident at an angle θ from the substrate region, as shown in Fig. 4. In this case, $k_{x0} = k_s \sin\theta$ refers to the wavenumber along x dictated by the incident wave and, in view of (3) in Section II, the fields in the substrate are given by

$$E_s = \exp(ik_{x0}x + ik_{z0}^{(s)}z) + \sum_n s_n \exp(ik_{xn}x - ik_{zn}^{(s)}z) \tag{33}$$

$$H_s = Y_0^{(s)} \exp(ik_{x0}x + ik_{z0}^{(s)}z) - \sum_n s_n Y_n^{(s)} \exp(ik_{xn}x - ik_{zn}^{(s)}z) \tag{34}$$

where it is assumed that the incident wave amplitude is unity and the amplitudes s_n of the scattered waves have to be determined. The fields in the air region are given by

$$E_a = \sum_n a_n \exp(ik_{xn}x + ik_{zn}^{(a)}z) \tag{35}$$

$$H_a = \sum_n a_n Y_n^{(a)} \exp(ik_{xn}x + ik_{zn}^{(a)}z) \tag{36}$$

where k_{xn} and $k_{zn}^{(j)}$ were defined in (4) and (6), $Y_n^{(j)}$ is now the characteristic modal admittance

$$Y_n^{(j)} = \begin{cases} k_{zn}^{(j)}/\omega\mu_0, & \text{for TE modes} \\ \omega\epsilon_0\epsilon_j/k_{zn}^{(j)}, & \text{for TM modes} \end{cases} \qquad (j \neq g) \tag{37}$$

and the amplitudes a_n are to be determined together with

s_n and $g_m^{(\pm)}$ by matching the boundary conditions, which require that the appropriate components in (29), (30), and (33)–(36) be continuous at $z = 0$ and t_g. This leads to the following systems of equations:

$$\delta_{0n} + s_n = \sum_m V_{mn}[g_m^{(+)} + g_m^{(-)}] \tag{38}$$

$$Y_n^{(s)}(\delta_{0n} - s_n) = \sum_m I_{mn}[g_m^{(+)} - g_m^{(-)}] \tag{39}$$

$$\sum_m V_{mn}[\exp(i\kappa_m t_g) g_m^{(+)} + \exp(-i\kappa_m t_g) g_m^{(-)}] = \exp(ik_{zn}^{(a)} t_g) a_n \tag{40}$$

$$\sum_m I_{mn}[\exp(i\kappa_m t_g) g_m^{(+)} - \exp(-i\kappa_m t_g) g_m^{(-)}] = \exp(ik_{zn}^{(a)} t_g) Y_n^{(a)} a_n \tag{41}$$

for all $n = 0, \pm 1, \pm 2, \cdots$. These are the four coupled systems of linear equations that determine the four sets of unknown scattered harmonic amplitudes a_n, s_n, $g_n^{(+)}$, and $g_n^{(-)}$, as follows.

Multiplying (40) by $Y_n^{(a)}$ and then subtracting the resulting equation from (41), we obtain, in matrix notation,

$$\boldsymbol{g}^{(-)} = \exp(i\boldsymbol{K}_g t_g) \boldsymbol{R}_g \exp(i\boldsymbol{K}_g t_g) \boldsymbol{g}^{(+)} \tag{42}$$

where $\boldsymbol{g}^{(\pm)}$ are column matrices with elements $g_m^{(\pm)}$, $\exp(i\boldsymbol{K}_g t_g)$ is a diagonal matrix with elements $\delta_{mn} \exp(i\kappa_m t_g)$ and $\boldsymbol{R}_g$ is the reflection coefficient matrix looking into the air region at $z = t_g$, as given by

$$\boldsymbol{R}_g = (\boldsymbol{I} + \boldsymbol{Y}_a \boldsymbol{V})^{-1} (\boldsymbol{I} - \boldsymbol{Y}_a \boldsymbol{V}) \tag{43}$$

with $\boldsymbol{I}$ and $\boldsymbol{V}$ being square matrices with elements $(\boldsymbol{I})_{mn} = I_{nm}$ and $(\boldsymbol{V})_{mn} = V_{nm}$, respectively, and $\boldsymbol{Y}_a$ being a diagonal matrix with elements $Y_n^{(a)} \delta_{mn}$.

Next, we multiply (38) by $Y_n^{(s)}$, add the result to (39) and invoke (42) to obtain

$$\boldsymbol{S}_g \boldsymbol{g}^{(+)} = \boldsymbol{T}_0 \boldsymbol{e} \tag{44}$$

with

$$\boldsymbol{S}_g = \boldsymbol{1} - \boldsymbol{R}_0 \exp(i\boldsymbol{K}_g t_g) \boldsymbol{R}_g \exp(i\boldsymbol{K}_g t_g) \tag{45}$$

$$\boldsymbol{T}_0 = 2(\boldsymbol{I} + \boldsymbol{Y}_s \boldsymbol{V})^{-1} \boldsymbol{Y}_s \tag{46a}$$

$$\boldsymbol{R}_0 = (\boldsymbol{I} + \boldsymbol{Y}_s \boldsymbol{V})^{-1} (\boldsymbol{I} - \boldsymbol{Y}_s \boldsymbol{V}). \tag{46b}$$

Here $\boldsymbol{e}$ is a column vector with elements δ_{0n}, $\boldsymbol{Y}_s$ is a diagonal matrix with elements $Y_n^{(s)} \delta_{mn}$, while $\boldsymbol{T}_0$ and $\boldsymbol{R}_0$ are, respectively, transmission and reflection matrices looking down into the substrate at $z = 0$.

When the matrix $\boldsymbol{S}_g$ in (44) is singular, the fields are in resonance as discussed in Section V. For nonresonant fields, the inverse of $\boldsymbol{S}_g$ exists and $\boldsymbol{g}^{(+)}$ is then uniquely determined via (44) for plane-wave incidence. Using (42) and (44), we then obtain from (38) that the scattered field amplitudes s_n in the substrate are given by the column vector

$$\boldsymbol{s} = \bar{\boldsymbol{R}}_0 \boldsymbol{e} \tag{47a}$$

where $\bar{\boldsymbol{R}}_0$ is a reflection matrix looking up at $z = 0$, as given by

$$\bar{\boldsymbol{R}}_0 = \boldsymbol{T}_0^{-1}[\exp(i\boldsymbol{K}_g t_g) \boldsymbol{R}_g \exp(i\boldsymbol{K}_g t_g) - \boldsymbol{R}_0] \boldsymbol{S}_g^{-1} \boldsymbol{T}_0. \tag{47b}$$

If required, the scattered amplitudes a_n in the air can be similarly obtained via (40) or (41), together with (42) and (44). This would complete the determination of all the scattered amplitudes a_n, $g_m^{(\pm)}$, and s_n.

V. THE FIELDS GUIDED BY DIELECTRIC GRATINGS

As discussed in the Introduction, the fields of greatest interest are those that can be supported by periodic thin-film structures in the absence of any wave incident from the air or the substrate. These fields are those of the surface and leaky waves described in Section II, which represent free-resonant solutions of the boundary-value problem under consideration. We shall discuss these solutions first for the canonic structure shown in Fig. 4, after which we shall generalize the result to structures with an arbitrary number of layers in addition to the single periodic layer of Fig. 4.

A. Guiding by a Single Periodic Layer

In the absence of a wave incident from an exterior region, we have a null vector instead of $\boldsymbol{e}$ in (44), which is then satisfied only if the determinant of $\boldsymbol{S}_g$ vanishes, namely,

$$\det(\boldsymbol{S}_g) = \det[\boldsymbol{1} - \boldsymbol{R}_0 \exp(i\boldsymbol{K}_g t_g) \boldsymbol{R}_g \exp(i\boldsymbol{K}_g t_g)] = 0. \tag{48}$$

This represents the dispersion relation for the guided (surface or leaky) waves of the grating in Fig. 4. This relation yields the unknown eigenvalues k_{x0}. For any such k_{x0}, we can then find all $g_n^{(+)}$ in terms of one of them by replacing $\boldsymbol{e}$ by $\boldsymbol{0}$ in (44). All of the other amplitudes a_n, $g_n^{(-)}$, and s_n can thereafter be determined as discussed at the end of the preceding section.

Because the foregoing analysis regards the fields as propagating along the z direction, which is normal to the boundaries, the result of (48) represents the transverse resonance condition for the present configuration. To understand the physical significance of this condition, let us consider the special case when the periodic layer in Fig. 4 is replaced by a uniform slab (with no periodic variation). In this case, (48) reduces to

$$1 - r_0 r_g \exp(2i\kappa t_g) = 0 \tag{49}$$

where r_0 and r_g are reflection coefficients looking into the substrate and air regions, respectively, at $z = 0$ and t_g. Equation (49) states the familiar (resonant, surface-wave) condition that the wave remains unchanged after a round-trip travel across the layer, the trip including one reflection at each of the two boundaries [21]. Thus (48) for the grating layer is a generalization of (49) for the uniform layer. The transition from scalars in (49) to matrices in (48) represents the fact that the presence of periodicity introduces energy coupling from the fundamental ($n = 0$) field to its higher order ($n \neq 0$) space harmonics.

In the case of a uniform layer, (49) is a transcendental equation, which may be solved graphically or numerically to find the propagation factor along the structure. For a periodic layer, (48) is considerably more complicated

because it involves an infinite determinant which must be truncated to solve for the unknown propagation factor k_{x0}. This determinant is also of the Hill's type, as was the case in (22), so that its truncation can be carried out very accurately by numerical computer techniques, as discussed further in Section VI.

B. Guiding by Multilayered Periodic Structures

The results discussed in the preceding section may now be extended to structures that possess several layers which are additional to the single nonuniform (periodic) layer discussed above. For this purpose, we first recognize that the electromagnetic problem of the single periodic layer may be rigorously described by the equivalent transverse network shown in Fig. 5(a). In this network, each of the semi-infinite transmission line in the air or substrate regions represents one of the modes; the characteristic admittance $Y_n^{(j)}$ and propagation factor $k_{zn}^{(j)}$ have been defined in (37) and (6), respectively. All of these transmission lines are connected to the grating region, which is now represented schematically by the box marked B in Fig. 5(a).

If desired, the network describing the scattering properties of the box marked B can be synthesized along the lines discussed in [22] for the case of an interface to a sinusoidally modulated medium. However, this synthesis is not necessary for the purposes of the present work because we may regard the box marked B in Fig. 5(a) to be defined by (47) for $\boldsymbol{S}_g$. We note, on the other hand, that the matrix $\boldsymbol{S}_g$ describes the coupling of all of the modes to each other via the periodic properties of the grating region.

To generalize the result to additional uniform layers, consider now the structures described in Fig. 1(a) and 1(b). These configurations can be represented by the equivalent network of Fig. 5(b), which is obtained by simply interposing an appropriate set of transmission lines of lengths t_f between the grating and substrate regions. In this case, we may look down at the plane $z = -t_f$ and define a reflection coefficient

$$\rho_n = \frac{Y_n^{(f)} - Y_n^{(s)}}{Y_n^{(f)} + Y_n^{(s)}}. \tag{50}$$

By utilizing ρ_n, we obtain that the input admittance $Y_n^{(in)}$ at $z = 0$ in every transmission line is given by

$$Y_n^{(in)} = \frac{1 - \rho_n \exp(2ik_{zn}^{(f)}t_f)}{1 + \rho_n \exp(2ik_{zn}^{(f)}t_f)} Y_n^{(f)}. \tag{51}$$

We can use now (45) for $\boldsymbol{R}_0$ and replace $Y_n^{(s)}$ therein with $Y_n^{(in)}$ to get the modified reflection matrix $\boldsymbol{R}_0'$ for the (two-layer) configurations of Fig. 1 in the form

$$\boldsymbol{R}_0' = (\boldsymbol{I} + \boldsymbol{Y}_{in}\boldsymbol{V})^{-1}(\boldsymbol{I} - \boldsymbol{Y}_{in}\boldsymbol{V}) \tag{52}$$

where $\boldsymbol{Y}_{in}$ is a diagonal admittance matrix with elements $Y_n^{(in)}\delta_{mn}$. By next taking $\boldsymbol{R}_0'$ instead of $\boldsymbol{R}_0$ in (48), the transverse resonance condition is extended to the geometries of Fig. 1, which possess the additional uniform layer of thickness t_f.

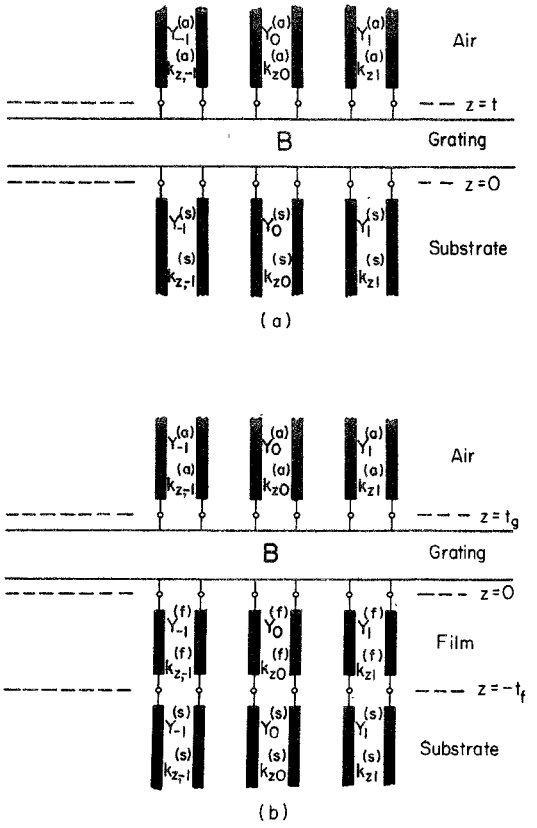

Fig. 5. Equivalent transverse networks for the analysis of dielectric-grating structures. (a) Network for the single-layer configurations of Fig. 3. (b) Network for the structures shown in Fig. 1.

The above procedure can, of course, be generalized to any number of layers that are added below the film layer. As suggested by Fig. 5, all that is needed is to modify $\boldsymbol{R}_0'$ so as to take into account the additional layers. As such a modified expression for $\boldsymbol{R}_0'$ involves the input admittances $Y_n^{(in)}$ looking into a stack consisting of an arbitrary number of uniform layers, the extension is straightforward. The same procedure can be utilized if additional uniform layers are placed above (rather than below) the grating region. In this case, the reflection matrix $\boldsymbol{R}_g$ must be modified to a matrix $\boldsymbol{R}_g'$ in a manner analogous to that discussed above for $\boldsymbol{R}_0'$. Of course, uniform layers may be accommodated both below and on top of the grating layer by employing the appropriate modified expressions $\boldsymbol{R}_0'$ and $\boldsymbol{R}_g'$ at the respective boundaries of the grating region.

Finally, additional periodic (rather than uniform) layers can also be accommodated in order to treat structures discussed in Section IIIC. This extension is somewhat more complicated because now we connect additional boxes of the form marked B in Fig. 5 rather than just transmission line sections. In matrix notation, this extension is nevertheless conceptually straightforward and the resulting expressions are relatively simple if all the periodic layers possess the same periodicity d, as prescribed in Section IIIC. As such an extension is beyond the scope of this paper, the interested reader should consult reference [23] for further details.

VI. DERIVATION OF NUMERICAL RESULTS

The application of the techniques described above involves the solution of the secular equation, which in this case is given by the vanishing of the infinite determinant of $\boldsymbol{S}_g$ in (45). We recall that all of the parameters entering into $\boldsymbol{S}_g$ are assumed known, except for k_{x0} which is regarded as the unknown variable for any given frequency ω. In general, however, the quantities κ_m and c_{mn} (in the grating region) are not known explicitly, so that the determination of their values is part of the computation process for finding k_{x0}.

A first step in the programming of a computer routine for solving the transverse resonance (secular) relation is to provide a subroutine for the calculation of κ_m and c_{mn} for any given combination of k_o and k_{x0}. As discussed in Section III, such a subroutine is generally dependent on the specific grating structure, but it usually involves the calculation of a suitably truncated determinant of the infinite matrix defined in (22). After finding the eigenvalues κ_m of this truncated matrix, the pertinent Fourier coefficients c_{mn} can be determined from their defining relation (21). Of course, the accuracy of all κ_m and c_{mn} is dependent on the order of the truncated determinant. In general, this accuracy increases with the order; as the determinant is of the Hill's type, the truncation needs not be unduly large for the accuracies required by practical considerations. However, great care must be exercised when choosing the rows and columns of the truncated determinant because an improper choice may considerably degrade the ultimate accuracy that is obtained. This is particularly true for calculations involving waves at or near a Bragg condition in the grating region, i.e., for values of $\beta_0 d = N\pi (N = \pm 1, \pm 2, \pm 3, \cdots)$. A discussion on this question for the specific case of a sinusoidally modulated medium is given in [22, appendix]; it is expected that the considerations presented there apply also to a more general variation of periodic variations.

The subroutine for determining all required κ_m and c_{mn} is then introduced into the program that handles the calculation of k_{x0}. As was the case for the subroutine, the program for finding k_{x0} also involves the calculation of a suitably truncated determinant of an infinite matrix $\boldsymbol{S}_g$, which is again of the Hill's type. Hence the considerations for truncating $\boldsymbol{S}_g$ are similar to those for the subroutine mentioned above. However, when solving for k_{x0} by using (48) for the truncated determinant, the computer calculation (usually involving Newton's iteration method) may converge very slowly This happens especially with configurations of the type shown in Fig. 1 for which the waveguiding process is primarily determined by the uniform layer rather than by the grating layer. In such cases, the calculation of k_{x0} is more easily and more accurately performed by utilizing another matrix $\boldsymbol{S}_f$ instead of $\boldsymbol{S}_g$.

This is obtained by noting from Fig. 5(b) that at $z = 0$ in the uniform layer, the field amplitudes $f_n^{(\pm)}$ are related by

$$\boldsymbol{f}^{(-)} = \hat{\boldsymbol{R}}_0 \boldsymbol{f}^{(+)} \tag{53}$$

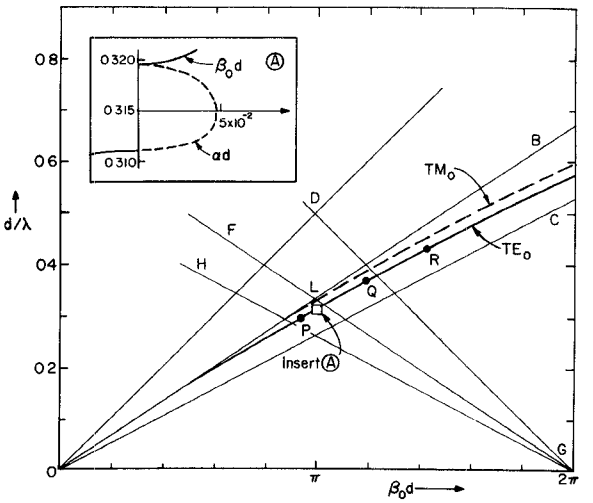

Fig. 6. Variation of $\beta_0 d$ for the fundamental TE and TM modes along a modulated layer as shown in Fig. 4 with $\epsilon_a = 1$, $\epsilon_g = 3.61$, $\epsilon_s = 2.25$, $M < 0.5$, and $t = 2d/\pi$. The insert shows the first stopband for $M = 0.08$.

where $\boldsymbol{f}^{(\pm)}$ are column vectors with elements $f_n^{(\pm)}$ and $\hat{\boldsymbol{R}}_0$ is given by $\bar{\boldsymbol{R}}_0$ in (47b) with the subscript s replaced by f in (46). On the other hand, at $z = -t_f$, the same amplitudes satisfy

$$f_n^{(+)} = \rho_n f_n^{(-)} \exp\,(i2k_{zn}^{(f)} t_f) \tag{54}$$

where ρ_n is given in (50). Inserting (54) into (53), we find

$$\boldsymbol{S}_f \boldsymbol{f}^{(+)} = [\boldsymbol{1} - \exp\,(i2\boldsymbol{k}_f t_f)\, \boldsymbol{R}_f \hat{\boldsymbol{R}}_0] \boldsymbol{f}^{(+)} = 0 \tag{55}$$

where $\boldsymbol{S}_f$ is defined by the matrix in the square brackets, $\exp\,(i2\boldsymbol{k}_f t_f)$ and $\boldsymbol{R}_f$ are diagonal matrices with elements $\delta_{mn} \exp\,(i2k_{zn}^{(f)} t_f)$ and $\delta_{mn}\rho_n$, respectively. Here $\det\,(\boldsymbol{S}_f) = 0$ expresses the transverse-resonance condition inside the film layer in a manner analogous to that whereby $\det\,(\boldsymbol{S}_g) = 0$ expresses this condition inside the grating layer.

By thus choosing a suitably truncated matrix $\boldsymbol{S}_f$ or $\boldsymbol{S}_g$, the computer program first finds k_{x0} by solving (48) or (55), after which the amplitudes a_n and s_n can be found by solving the simultaneous set of equations (38)–(41). The values of $k_{x0} = \beta_0 + i\alpha$, together with the magnitudes of all a_n and s_n, usually complete the information needed for the design of a particular dielectric grating structure.

To illustrate some of the results that can be obtained by the techniques discussed above, we present below several calculated curves for gratings of the type shown in Figs. 1(b) and 4.

The Brillouin diagram for a modulated layer is given in Fig. 6 for the lowest (fundamental) TE_0 and TM_0 modes. As predicted by the argument given in connection with Fig. 2, these dispersion curves show that the wavenumber β_0 is very closely equal to the value β_{sw} of the surface wave along a uniform ($M = 0$) layer. In fact, for values of $M \leq 0.5$, it is not possible to distinguish β_0 from β_{sw} on the scale of Fig. 6. In agreement with the theory of surface waves along uniform layers [21], the dispersion curves in Fig. 6 lie between the straight lines OB and OC

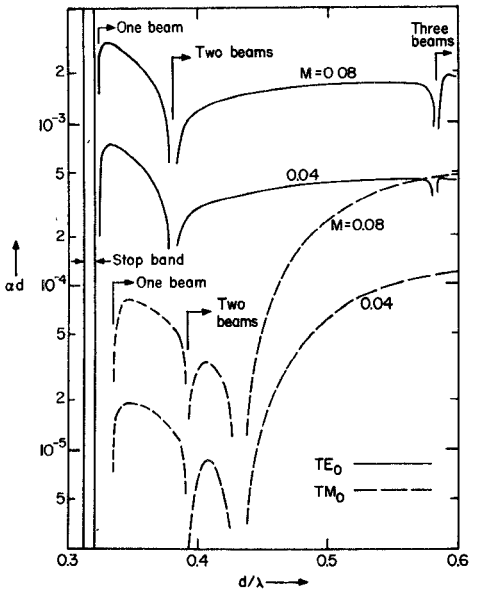

Fig. 7. Variation of the attenuation parameter α with frequency for the same grating as that in Fig. 6. The range shown allows for either a single beam in the substrate (e.g., point Q in Fig. 6) or for two beams, one each in the substrate and air regions (e.g., point R in Fig. 6). Inside the stopband, α becomes very large and reaches a peak which is well outside the vertical range shown.

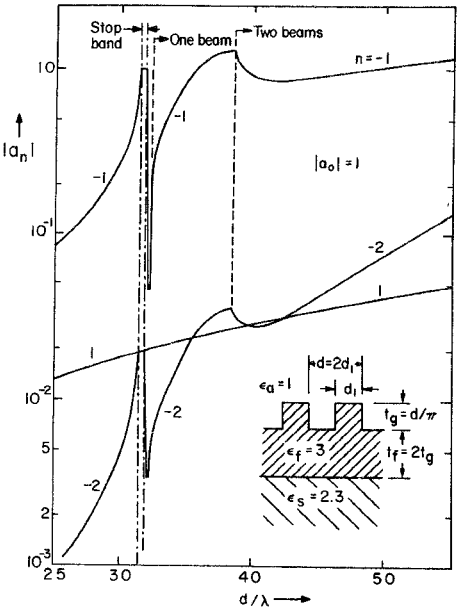

Fig. 8. Variation of the space-harmonic amplitudes a_n with frequency for the TE_0 made along a rectangular grating.

through the origin, whose slope is given by $\cot^{-1}(\epsilon_s^{1/2})$ and $\cot^{-1}(\epsilon_g^{1/2})$, respectively.

The presence of periodicity manifests itself most strongly by causing stopbands at frequencies for which a Bragg condition $\beta_0 d = N\pi (N = \pm 1, \pm 2, \cdots)$ is satisfied. Such a stopband region is illustrated in Fig. 6 by insert A, which shows both $\beta_0 d$ and αd around $\beta_0 d = \pi$ in magnified form. For wavelengths λ inside this stopband, the field of the surface wave is in the form of a decaying standing-wave with respect to the x direction.

Besides producing stopbands, the presence of periodicity may also change the surface waves into leaky waves, as discussed in Section II. To assess this, we reflect the lines OB and OC about $\beta_0 d = \pi$ to obtain FG and HG. By taking into account the slopes of the various lines in conjunction with (6), we may verify that, for $j = a$ and s, all $k_{zn}^{(j)}$ are pure imaginary *inside* the triangular region OLG. However, $k_z^{(s)}$ is real *outside* this triangle, whereas both $k_{z,-1}^{(s)}$ and $k_{z,-1}^{(a)}$ are real outside the larger triangular region OLG. Thus at frequencies for which the operation point is inside the smaller triangle OLG (e.g., point P), the surface wave remains bound even if periodicity is present. As frequency increases and the operation point crosses the line FG (e.g., point Q), a radiation beam occurs in the substrate and the surface wave is changed to a leaky wave. For frequencies that are high enough so that the operating point is above the DG line (e.g., point R), radiation beams occur in both substrate and air regions.

The attenuation parameter α, which is due either to a stopband or to power leakage, is shown in Fig. 7. As frequency varies, α starts by being zero in the surface-wave region; however, α is nonzero and peaks strongly in the stopband region. This stopband behavior is of importance in the operation of distributed-feedback lasers and the maximum value of α determines the length required for effective lasing conditions. Outside the stopband, α is nonzero if the frequency is high enough to produce radiation, i.e., the wave is leaky. As seen in Fig. 7, α varies slowly with frequency in the leaky-wave region, except in the vicinity of certain critical values of d/λ. These critical values of d/λ are associated with the presence of Wood's anomalies along gratings [24]; in the present case, these correspond to the onset of additional leaky-wave beams in the air or substrate regions. However, for TM modes, additional nulls may appear for α, which are due to a Brewster-angle phenomenon for a higher ($n \neq 0$) harmonic inside the grating layer. Such a case is shown by the null in α for TM_0 at about $d/\lambda = 0.43$.

For both surface-wave and leaky-wave applications, the amplitudes a_n are of great interest because their magnitudes determine the efficiency of devices that employ waves guided by periodic structures. We therefore show in Fig. 8 the variation of a_{-2}, a_{-1}, and a_1 (with $a_0 = 1$) for the fundamental TE_0 mode along a rectangular grating of the type shown in Fig. 1(b). We recall that a_n denotes the amplitude of the nth space harmonic at the air-grating boundary $z = t_g$. As the Brillouin diagram is basically similar to that already given in Fig. 6, it is omitted here, but its pertinent stopband and leaky wave regions are indicated in Fig. 8. It is noted that the curves for a_n undergo rapid variations close to the stopband edges. Also, we note that $|a_{-1}| = a_0 = 1$ and $|a_{-2}| = |a_1|$ within the stopband, in agreement with the fact that the field is a standing wave in the stopband.

Although some of the foregoing curves could have been calculated by the approximate techniques reported in the past [2]–[5], [7]–[9], [12], their accuracy should be checked by a rigorous method such as that presented here. To show the importance and the generality of the method discussed in this paper, we show in Fig. 9 the variation of α for the same grating as that of Fig. 8, except that now the wavelength λ is assumed fixed and the grating thickness

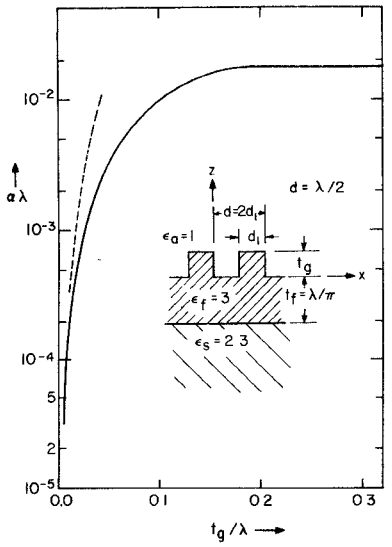

Fig. 9. Variation of α with the grating thickness t_g for the same grating as in Fig. 8. The solid curve shows the exact result whereas the dashed line refers to a result obtained by a perturbation analysis.

t_g varies. In this case, a perturbation analysis [5] would yield the dashed curve, for which α increases continuously with t_g. In contrast, our rigorous treatment yields the solid curve, which indicates that $\alpha\lambda$ reaches a saturation value close to 0.02 for values of $t_g/\lambda > 0.2$.

The behavior of the solid curve in Fig. 9 can easily be explained by noting that the basic surface wave along a uniform ($t_g = 0$) layer has an evanescent field in the air region. When increasing t_g from zero, we perturb this surface wave field by adding material on top of the uniform film of thickness t_f. At first, this material appears in a region with strong fields and therefore the effect on α is appreciable. However, as t_g increases further, the additional material appears in regions where the field has gradually decayed until, at about $t_g/\lambda = 0.2$, any further addition of material occurs in regions where the field is exponentially small. Consequently, the effect of increasing t_g beyond 0.2λ is negligible and α approaches a constant.

The above is only one example of the serious discrepancies that may occur between an exact result and that obtained by approximate techniques. Although the method presented here may be somewhat cumbersome to use, such a method is essential if one wishes to verify the validity of simpler but approximate results of unknown accuracy.

ACKNOWLEDGMENT

The authors wish to thank Prof. R. Petit, The University of Aix-Marseille III, France, for his constructive criticism of the first manuscript, and Mrs. Ida Tobiason for the patient and careful typing of the several versions of this work.

REFERENCES

[1] T. Tamir and H. L. Bertoni, "Lateral displacement of optical beams at multilayered and periodic structures," *J. Opt. Soc. Amer.*, vol. 61, pp. 1397–1413, Oct. 1971.
[2] L. L. Hope, "Theory of optical grating couplers," *Opt. Commun.*, vol. 5, pp. 179–182; June 1972.
[3] J. A. Harris, R. K. Winn, and D. G. Dalgoutte, "Theory and design of periodic couplers," *Appl. Opt.*, vol. 11, pp. 2234–2241, Oct. 1972.
[4] F. W. Dabby, A. Kestenbaum, and U. C. Paek, "Periodic dielectric waveguides," *Opt. Commun.*, vol. 6, Oct. 1972.
[5] K. Ogawa, W. S. C. Chang, B. L. Sopori, and F. J. Rosenbaum, "A theoretical analysis of etched grating couplers for integrated optics," *IEEE J. Quantum Electron. (Part I of Two Parts)*, vol. QE-9, pp. 29–42, Jan. 1973.
[6] S. T. Peng, T. Tamir, and H. L. Bertoni, "Leaky-wave analysis of optical periodic couplers," *Electron. Lett.*, vol. 9, pp. 150–152, Mar. 1973.
[7] C. Elachi and C. Yeh, "Frequency selective coupler for integrated optics systems," *Opt. Commun.*, vol. 7, pp. 201–204, Mar. 1973.
[8] K. Sakuda and A. Yariv, "Analysis of optical propagation in a corrugated dielectric waveguide," *Opt. Commun.*, vol. 8, pp. 1–4, May 1973.
[9] H. Stoll and A. Yariv, "Coupled-mode analysis of periodic dielectric waveguides," *Opt. Commun.*, vol. 8, pp. 5–8, May 1973.
[10] (a) N. Neviere, R. Petit, and M. Cadilhac, "About the theory of optical grating coupler-waveguide systems," *Opt. Commun.*, vol. 8, pp. 113–117, June 1973.
(b) M. Neviere, P. Vincent, R. Petit, and M. Cadilhac, "Systematic study of resonance of holographic thin film couplers," *Opt. Commun.*, vol. 9, pp. 48–53, Sept. 1973.
(c) ——, "Determination of the coupling coefficient of a holographic thin film coupler," *Opt. Commun.*, vol. 9, pp. 240–245, Nov. 1973.
[11] C. Elachi and C. Yeh, "Periodic structures in integrated optics," *J. Appl. Phys.*, vol. 44, pp. 3146–3152, July 1973.
[12] K. Ogawa and W. S. C. Chang, "Analysis of holographic thin film grating coupler," *Appl. Opt.*, vol. 12, pp. 2167–2171, Sept. 1973.
[13] S. T. Peng, H. L. Bertoni, and T. Tamir, "Analysis of periodic thin-film structures with rectangular profile," *Opt. Commun.*, vol. 10, pp. 91–94, Jan. 1974.
[14] S. T. Peng, T. Tamir, and H. L. Bertoni, "Analysis of thick-grating beam couplers," in *Digest Tech. Papers, Topical Meeting on Integrated Optics*, pp. TuB8-1–TuB8-4, Jan. 1974.
[15] L. V. Kantorovich and V. I. Krilov, *Appropriate Methods of Higher Analysis*. New York: Interscience, 1958, sec. I.3, p. 26.
[16] T. Tamir, H. C. Wang, and A. A. Oliner, "Wave propagation in sinusoidally stratified dielectric media," *IEEE Trans. Microwave Theory Tech.*, vol. MTT-12, pp. 323–335, May 1964.
[17] H. C. Wang, "Electromagnetic wave propagation along a sinusoidally stratified dielectric slab," Ph.D. dissertation, Polytechnic Institute of Brooklyn, New York, N.Y., 1965.
[18] C. Yeh, K. F. Casey, and Z. A. Kaprelian, "Transverse magnetic wave propagation in sinusoidally stratified dielectric media," *IEEE Trans. Microwave Theory Tech.*, vol. MTT-13, pp. 297–302, May 1965.
[19] S. T. Peng and A. Hessel, "Generalized continued fractions in electromagnetic problems," presented at the URSI Meeting, Boulder, Colo., Aug. 1973, to be published.
[20] L. R. Lewis and A. Hessel, "Propagation characteristics of periodic arrays of dielectric slabs," *IEEE Trans. Microwave Theory Tech.*, vol. MTT-19, pp. 276–286, Mar. 1971.
[21] T. Tamir, "Inhomogeneous wave types at planar interfaces: II. Surface waves," *Optik*, vol. 37, pp. 204–228, Sept. 1973.
[22] ——, "Scattering of electromagnetic waves by a sinusoidally-stratified half space, Part II: diffraction aspects at the Rayleigh and Bragg wavelengths," *Can. J. Phys.*, vol. 44, pp. 2461–2494, Oct. 1966.
[23] S. T. Peng and T. Tamir "Effects of groove profile on the performance of dielectric grating couplers," in *Proc. Symp. Optical and Acoustical Micro-Electronics*. Brooklyn, N.Y.: Polytechnic Press, 1974.
[24] A. Hessel and A. A. Oliner, "A new theory of Wood's anomalies on optical gratings," *Appl. Opt.*, vol. 4, pp. 1275–97, Oct. 1965.
[25] R. E. Collin and F. J. Zucker, Eds., *Antenna Theory*, vol. 2. New York: McGraw-Hill, 1969, sec. 19.10, p. 203.